Auger Line-Shape Studies of the Bonding Transition-Metal Carbonyls and Nitrosyls†

G. D. Stucky,‡ R. R. Rye,* D. R. Jennison, and J. A. Kelber

Contribution from the Sandia National Laboratories, Albuquerque, New Mexico 87185.
Received September 25, 1981

Abstract: We have obtained and theoretically analyzed the C, N, and O core–valence–valence Auger spectra of CO, NO, $Co(CO)_3NO$, $Fe(CO)_5$, and $Mo(CO)_6$. These spectra are shown to have a qualitative chemical interpretation in terms of ground-state molecular orbital (MO) descriptions. The involvement of both core and valence electrons in the Auger process causes a sensitivity to the valence electron density in the immediate vicinity of the atom containing the initial core hole. As a result, the variation in relative intensity of transitions for different atomic sites in a molecule is a measure of the polarization of the orbital electron density distribution. The nitrogen and oxygen spectra of NO are far more similar than the carbon and oxygen spectra of CO, reflecting a more equal electron density distribution of the valence MO's. Another major difference between the spectra of NO and CO is the presence of peaks corresponding to transitions involving the 2π level of NO. A common fingerprint carbon Auger spectrum is obtained for the metal carbonyls that is independent of the central metal atom. The carbon and oxygen spectra largely result from CO-like orbitals with a final-state hole–hole repulsion comparable to that in free CO, indicating that the final-state holes are localized on the carbonyl group containing the initial core hole. The carbon spectrum of the metal carbonyls differs from that of free CO in that a peak occurs in the carbonyl spectra the intensity of which is due to fractional occupancy of the 2π level. This occupancy results from a screening charge that flows from the metal atom in response to creation of the initial-carbon core hole and that increases the $d\pi$–$p\pi$ backbonding. Theoretical analysis of the carbonyl Auger spectra, which are directly sensitive to the local-valence charge density, indicates that ab initio Hartree–Fock calculations performed with double-ζ basis sets predict an electron density that is in agreement with the experimental Auger results. The assignment of the lowest energy and highest amplitude $C(1s^{-1})$ core-hole state in carbonyls (the subject of some recent debate) was checked as different Auger initial states lead to very different Auger line shapes. It is found that the adiabatically relaxed state (as opposed to a shakeup state) dominates.

In order to understand and predict chemical processes, it is important to be able to monitor the local-valence-electronic properties at atomic sites within a molecular species. It is this information that enables one to define how a molecule will respond to nucleophilic or electrophilic attack both with respect to specifying the point of attack within a molecule and the ways in which one might modify that site to enhance or decrease its chemical reactivity.

The experimental difficulties in unambiguously defining local electronic properties are considerable and have led to an extensive literature concerning questions such as the nature of five-coordinate (or higher) carbon atoms in electron-deficient main-group chemistry, bent bonds and the relatively high reactivity of small strained rings, alkyl C–H bond activation, the consequences of $p\pi$–$d\pi$ bonding in silicon chemistry, and the activation of dinitrogen and carbon monoxide for hydrogenation. From both a practical and basic research point of view, another area currently of particular interest is the delineation of the interactions of adsorbed molecules with surfaces. Experimental information regarding the specific mode of interaction and its effect on molecular properties is especially important to many processes, including catalysis, corrosion, adhesion, and numerous other gas- and liquid-phase/solid-state phenomena. Obtaining these data is understandably even more difficult than for homogeneous systems.

Auger electron spectroscopy (AES) which has been extensively employed for elemental identification of surface species, has experienced recent rapid development as a spectroscopic technique that probes the local-valence electronic structure of molecules and solids.[1-4] The initial state for the Auger process is a core hole generated by electron, X-ray, or even ion impact. For the cases discussed in the present paper, the core hole is created by electron impact in a carbon, nitrogen, or oxygen atom K shell. This initial state decays via an electronic transition from one of the higher lying electron orbitals coupled with the ejection of a secondary (Auger) electron. If the two less tightly bound electrons are valence electrons, the overall process is labeled KV_1V_2, where V_1 and V_2 are valence levels.

The direct coupling of core and valence levels means that AES is a *local-valence-level* probe. Although complicated in that it is a two-electron process, AES potentially combines some of the attractive features of both core-level X-ray photoelectron spectroscopy (XPS) and valence-level ultraviolet photoelectron spectroscopy (UPS). The utilization of AES to probe valence electronic structure requires a theoretical treatment of the final state of the KVV transition, which involves two interacting holes in the valence levels. A rigorous handling of this problem would involve a many-body calculation, which is impractical for all but the simplest molecules. However, the recent development of a relatively simple one-electron molecular-orbital approach[5-8] permits the elucidation of those physical processes that determine the detailed structure of Auger spectra.[5] A description of the one-electron molecular-orbital approach and the physical assumptions that allow its application to the Auger process is presented in the Theory section.

One important point from the chemist's point of view is that the KVV Auger transition intensity is a measure of the valence charge available for decay into the core hole. Because of the localized nature of the core-hole wave function, only charge in the immediate vicinity of the core hole contributes significantly to this decay.[9,10] Hence, unlike UPS, in which the valence electrons of all the atoms in the molecule contribute to the signal, the Auger line shape is a sensitive function of the valence-orbital

†This work was supported by the U.S. Department of Energy under Contract DE-AC04-76-DP00789. Sandia National Laboratories is a U.S. Department of Energy Facility.
‡Present address: E. I. du Pont de Nemours & Co., Inc., Wilmington, DE.

(1) Rye, R. R.; Madey, T. E.; Houston, J. E.; Holloway, P. H. *J. Chem. Phys.* **1978**, *69*, 1504.
(2) Netzer, F. P.; Matthew, J. A. D. *J. Electron Spectrosc. Relat. Phenom.* **1979**, *16*, 359.
(3) Rye, R. R.; Houston, J. E.; Madey, T. E.; Holloway, P. H. *Ind. Eng. Chem. Prod. Res. Dev.* **1979**, *18*, 2.
(4) Jennison, D. R. *Phys. Rev. B: Condens. Matter* **1978**, *18*, 6865.
(5) Jennison, D. R. *J. Vac. Sci. Technol.* **1980**, *17*, 172.
(6) Jennison, D. R. *Phys. Rev. A* **1981**, *23*, 1215.
(7) Jennison, D. R. *Chem. Phys. Lett.* **1980**, *69*, 435.
(8) Siegbahn, H.; Asplund, L.; Kelfve, P. *Chem. Phys. Lett.* **1975**, *35*, 330.
(9) Jennison, D. R. *Phys. Rev. Lett.* **1978**, *40*, 807.
(10) Matthew, J. A. D.; Komninos, Y. *Surf. Sci.* **1975**, *53*, 716.

0002-7863/82/1504-5951$01.25/0

electronic structure in the immediate vicinity of the atom on which the core hole is localized.[4]

The application of Auger line-shape analysis to molecules made up of the second-row elements carbon, nitrogen, and oxygen has resulted in particularly useful experimental information concerning the atomic-site valence-electron character of small strained-ring compounds,[11] alkanes,[12] ammonia adsorbed on Al_2O_3,[13] and nitriles.[14] AES spectral analysis has clearly shown that the carbon atom hybridization systematically changes from being nearly sp^2 in cyclopropane to sp^3 in cyclohexane.[11] The spectral contributions from terminal methyl carbon atoms and interior methylene carbon atoms are seen in the normal alkane series.[12] The effects of coordination of the lone-pair electrons of the NH_3 group to alumina is found to rationally change the N(KVV) Auger line shape.[13] The C(KVV) spectrum of CH_3CN is readily described in terms of the relatively independent contributions of an acetylenic-like sp-hybridized carbon atom and a methyl, sp^3-hybridized carbon atom while the N(KVV) spectrum of CH_3CN is dinitrogen-like.[14]

Recently we have initiated an effort to expand these investigations to probe chemical bonding between second-row and heavier elements. One especially important problem in this area is the characterization of metal–carbonyl interactions in transition-metal carbonyls, materials of interest in their own right and as models for CO chemisorption. The historical difficulties mentioned above in defining local electronic properties are especially well evidenced for this class of compounds by the extensive theoretical and experimental discussion[15-34] that still exists concerning the role of π backbonding and the interpretation of features observed in the X-ray photoelectron spectra of the carbon and oxygen 1s levels. The potential importance of AES for the study of adsorbed species in heterogeneous reactions is exemplified by the recent AES study of CO hydrogenation on a nickel surface.[35] This study has revealed both active carbidic carbon atom species and inactive graphitic carbon, the latter being formed to a greater extent at higher temperatures. Thus, AES has the capability of giving information about the valence electronic structure of the carbon atom in active surface intermediates in heterogeneous catalytic reactions. The detailed interpretation of spectra obtained from structurally related molecules in the gas phase is important in order to quantitatively analyze these data. The results presented here and in a previous preliminary report[36] from gas-phase studies of CO, NO, and a series of transition-metal carbonyls, $Mo(CO)_6$, $Fe(CO)_5$ and $Co(CO)_3NO$, are directed toward that goal as well as to a clarification of the bonding in metal carbonyls and nitrosyls.

Experimental Section

The apparatus used in the present work consists of a retarding, single-pass cylindrical mirror analyzer (CMA)[37] modified to have a molecular-jet and an electron-beam intersect at the analyzer focal point. The molecular jet is coaxial with the CMA axis and pointed away from the analyzer so that the exiting gas passes directly into a liquid nitrogen trapped, 2000 L/s oil diffusion pump. The electron beam is directed across the face of the CMA and proceeds directly into a Faraday cup. At the intersection of the electron beam and molecular jet, the molecular density is estimated to be ~200 times that indicated by the quiescent chamber pressure, which normally is held at $\sim 5 \times 10^{-5}$ torr.

CO and NO were used directly from compressed gas tanks without further purification. $Mo(CO)_6$, $Fe(CO)_5$, and $Co(CO)_3NO$ were purchased from Alfa Ventron Corp. and were purified by sublimation and/or distillation. The gas-phase purity within the Auger spectrometer was monitored with an UTI quadrupole mass analyzer. Sublimation of the $Mo(CO)_6$ during the experiment was at 10^{-5} torr and 30–35 °C, accomplished by maintaining the chamber containing the analyzer and a shortened version of the gas line at the sublimation temperature.

The spectra were acquired in multiple 100-eV energy scans by using a signal averager and relayed to a computer for processing and plotting. The individual Auger features were often found to reside on a slight background due to inelastic electron scattering from various exposed analyzer components, and this was removed by a simple linear-background-subtraction scheme.[1] The energy scale was calibrated relative to the major Auger peak of methane taken to be at 249-eV kinetic energy.[1,3]

Theory

It is clear that one would prefer to describe Auger spectra in terms of ground-state MO's since such one-electron approaches are easier to use and more widely understood than many-electron approaches. In addition, this would allow one to gain insight from Auger spectra into ground-state properties of molecular systems. However, since the Auger final state involves two holes (a +2 ion), the possibility of describing the Auger spectra in terms of ground-state MO's depends upon the degree of correlation between the final-state holes. If the holes are independent, the energy of the two-hole Auger final states will be given by a self-convolution of one-hole photoemission final states adjusted for the average hole–hole interaction energy (U_{eff}). For independent particle behavior, U_{eff} is approximately given by a Coulomb interaction integral using ground-state wave functions.[7] However, numerous examples for both metals[38,39] and molecules[12,40] have been seen where values of U_{eff} are observed that are much larger than expected from Coulomb interaction integrals. In these cases, the two final-state holes that are created together via the Auger decay process are highly correlated and remain together. For these final states, the holes are clearly not independent and a one-electron description is not appropriate. The proper description of such localized behavior is an active current area of theoretical research in Auger spectroscopy, and much insight has been recently generated.[41]

Independent motion of the holes requires that the energy of two (screened) holes upon one site (E_L) must be not very different from the energy of two holes upon separate sites (E_D) when compared to the magnitude of the off-diagonal Hamiltonian matrix element between the configurations of two holes on one site and holes on adjacent sites.[40] The latter matrix element is basically an interatomic interaction such as, for example, leads to the splitting (W) of the one-electron bonding and antibonding MO's. If $E_L - E_D \equiv \Delta U$ is small compared to W, the independent-hole model is valid. Such is the case with CO (ΔU is small, largely

(11) Houston, J. E.; Rye, R. R. *J. Chem. Phys.* **1981**, *74*, 71.
(12) Rye, R. R.; Jennison, D. R.; Houston, J. E. *J. Chem. Phys.* **1980**, *73*, 4867.
(13) Campbell, C. T.; Rogers, J. W., Jr.; Hance, R. L.; White, J. M. *Chem. Phys. Lett.* **1980**, *69*, 430.
(14) Rye, R. R.; Houston, J. E. *J. Chem. Phys.* **1981**, *75*, 2085.
(15) Bor, G. *J. Organomet. Chem.* **1967**, *10*, 343.
(16) Mann, R. H.; Hyams, I. J.; Lippincott, E. R. *J. Chem. Phys.* **1968**, *48*, 4929.
(17) Jones, L. H.; Swanson, B. I. *Acc. Chem. Res.* **1976**, *9*, 128.
(18) Beach, M. A.; Gray, H. B. *J. Am. Chem. Soc.* **1968**, *90*, 5713.
(19) Plummer, E. W.; Salaneck, W. R.; Miller, J. S. *Phys. Rev. B: Solid State* **1978**, *18*, 1673.
(20) Bancroft, G. M.; Boyd, B. D.; Creber, D. K. *Inorg. Chem.* **1978**, *17*, 1008.
(21) Caulton, K. G.; Fenske, R. F. *Inorg. Chem.* **1969**, *7*, 1273.
(22) Hillier, I. H.; Saunders, V. R. *Mol. Phys.* **1971**, *22*, 1025.
(23) Johnson, K. H.; Wahlgren, U. *Int. J. Quantum Chem., Symp.* **1972**, *6*, 243.
(24) Baerends, E. J.; Ros, P. *Mol. Phys.* **1975**, *30*, 1735.
(25) Johnson, J. B.; Klemperer, W. G. *J. Am. Chem. Soc.* **1977**, *99*, 7132.
(26) Messmer, R. P.; Lamson, S. H. *Chem. Phys. Lett.* **1979**, *65*, 465.
(27) Loubriel, G. Ph.D. Thesis, Department of Physics, University of Pennsylvania, 1979.
(28) Loubriel, G. *Phys. Rev. B: Condens. Matter* **1979**, *20*, 5339.
(29) Larsson, S.; Braga, M. *Int. J. Quantum Chem.* **1979**, *15*, 1.
(30) Bursten, B. E.; Freier, D. G.; Fenske, R. F. *Inorg. Chem.* **1980**, *19*, 1810.
(31) Sherwood, D. E.; Hall, M. B. *Inorg. Chem.* **1980**, *19*, 1805.
(32) Chen, H. D.; Jolly, W. L. *Inorg. Chem.* **1979**, *18*, 10.
(33) Avanzino, S. C.; Bakke, A. A.; Chen, H. W.; Donahue, C. J.; Jolly, W. L.; Lee, T. H.; Ricco, A. J. *Inorg. Chem.* **1980**, *19*, 1931.
(34) Davenport, J. V. *Chem. Phys. Lett.*, in press.
(35) Goodman, D. W.; Kelley, R. D.; Madey, T. E.; Yates, J. T., Jr. *J. Catal.* **1980**, *63*, 226.
(36) Jennison, D. R.; Stucky, G. D.; Rye, R. R.; Kelber, J. A. *Phys. Rev. Lett.* **1981**, *46*, 911.
(37) Gerlach, R. L.; Tipping, D. W. *Rev. Sci. Instrum.* **1971**, *42*, 1519.
(38) Sawatzky, G. A. *Phys. Rev. Lett.* **1977**, *39*, 504.
(39) Cini, M. *Solid State Commun.* **1977**, *24*, 681.
(40) Jennison, D. R.; Kelber, J. A.; Rye, R. R. *Phys. Rev. B: Condens. Matter* **1982**, *25*, 1384.
(41) For a review of Auger theory, see: Jennison, D. R. *J. Vac. Sci. Technol.* **1982**, *20*, 548.

due to geometry), and the intersite interaction is strong due to the triple bond.[42] In F_2, however, the bond distance is larger than in CO (smaller splitting and larger ΔU), and as a result $\Delta U/W$ should be larger for F_2 than for CO. Strong correlation effects between the final-state holes in the case of F_2 have been observed.[43]

We anticipate that due to the comparatively weak ligand–ligand interaction in the carbonyls (small W) and to the molecular size (the energy of two holes on one CO would be quite different than the energy of separated holes), strong hole–hole correlation effects would be likely to occur and many Auger final states would be highly correlated. The two-hole excitation spectrum of the system then, in general, separates into two regions: if the holes are created apart, they almost never come together (delocalized excitations); if they are created together (e.g., via Auger decay), then they cannot separate until the energy to be gained by separation is given to a third particle (VVV Auger). Since this process takes time, these most highly correlated two-particle excitations will be quite visible in an Auger spectrum. We call the latter states, in which the holes hop together from site to site, localized as their lifetime upon one site is, in general, much longer than single-hole lifetimes. However, even for the case where the holes are localized within a functional group (e.g., $-CH_3$),[40] an independent-hole description still may be a valid approximation when expressed in terms of functional-group orbitals (e.g., NiCO orbitals vs. $Ni(CO)_4$).

In the present case we will begin with the independent-particle MO approach. We will find that it works well for isolated CO, and we will point out necessary modifications in order to treat the carbonyls. Since the components of this approach have been given in detail previously,[6,7,42,44] only a brief summary will be presented here. The experimentally observed kinetic energy of the Auger electron is the difference between the initial- and final-state energies, E_i and E_f, respectively. The initial-state energy is given by eq 1 where E_0 is the ground-state energy of the molecule

$$E_i = E_0 + I_c \tag{1}$$

and I_c is the core ionization potential. The final state involves (by the independent-particle assumption) independent holes in the j and k molecular orbitals (MO's) with spin s so that

$$E_f(j,k,s) = E_0 + I_j + I_k + U_{eff}(j,k,s) \tag{2}$$

where I_j and I_k are the appropriate valence vertical ionization potentials. U_{eff} is defined according to the relation:

$$U_{eff} = R(j,k) - S(j,k) \tag{3}$$

where $R(j,k)$ is the bare hole–hole repulsion[45] and $S(j,k)$ is the interaction of one hole with the polarization field induced by the other.[46] For uncorrelated hole motion in delocalized molecular orbitals, $S(j,k)$ can generally be neglected.[7] However, when both holes are in spatially restricted lone-pair orbitals, $S(j,k)$ may be an appreciable part of U_{eff}.[6,42] Since we neglect $S(j,k)$ in our calculations, experimental energies for such (lone pair)$^{-2}$ final states may differ by several electron volts from calculated values but will always be smaller since S is positive.[46]

In order to include, at least approximately,[7] *single*-hole relaxation and correlation effects, we use experimental-core and valence-level vertical ionization potentials. By taking I_j to be independent of the presence or absence of the kth electron, we include all final-state two-hole effects in experimental values of U_{eff}.

As mentioned above, we will find that localization of the final-state holes occurs for the carbonyls and nitrosyls. However, because these molecules have relatively weak coupling between the CO-like and NO-like MO's, and since the independent-hole description is valid for isolated CO and NO (see below), once we establish localization we may theoretically treat the Auger final state in the carbonyls by using a molecular fragment such as NiCO. Because of the relatively weak coupling between the metal and ligand orbitals, we will describe the NiCO orbitals by their parentages, i.e., 3σ, 4σ, 1π, 5σ, $3d_\sigma$, $3d_\pi$, and $3d_\delta$, where the latter reflect the symmetry of the 3d orbital in the NiCO fragment. This description has the additional advantage of allowing easy visualization of the nature of the bonding.

The amplitude of the Auger signal is an important aspect of the data that is particularly useful in defining the valence electronic properties. The Auger transition probabilities are given by transition matrix elements between the initial-core-hole states and the two-hole final states.[6] The theoretical analysis reveals that the intensity is mainly a function of the core-hole initial-state valence atomic charge densities. However, the relaxation of the electron density due to the presence of the core hole is reflected in the nonorthogonality between initial- and final-state valence orbitals. This nonorthogonality is particularly important when the creation of the core hole breaks the ground-state molecular symmetry and results in mixing of orbitals that belong to different representations in the ground state.[6,42] An outline of the theoretical treatment of transition probabilities is given in the Appendix. The results may be summarized by the expression

$$I_{jk} \propto |\sum_{lm} C_{jk,lm} \sum_{\mu\nu} c_{l\mu}{}^* c_{m\mu} (c\mu|a\nu)|^2 \tag{4}$$

Here $C_{jk,lm}$ is a projection coefficient that accounts for the nonorthogonality between initial-state MO's l and m and final-state hole orbitals j and k. In the carbonyl case, our calculations show that $C_{jk,lm} \approx \delta_{jl}\delta_{km}$; i.e., nonorthogonality is not very important (typical coefficients are 0.95–0.98). In this case, eq 4 reduces to a product of the LCAO coefficients, $c_{l\mu}{}^* c_{m\nu}$, which may be interpreted in terms of the initial-state charge populations contributed by the local basis functions μ and ν and atomic-like Auger matrix elements $(c\mu|a\nu)$ over the local basis functions. Since the atomic-like matrix elements make a rather constant contribution for a particular angular momentum (i.e., 2s- vs. 2p-like), we may compare the relative amplitude of two shallow valence decays (all holes locally 2p-like) in terms of the atomic populations. Thus tables of initial-state atomic charge, in the absence of pronounced nonorthogonality, are helpful in understanding the Auger spectra. We note that the intensity scales as the *product* of the local atomic charge populations.

An important aspect of the Auger analysis is the relationship between the valence electron properties of the neutral-parent molecular species and the experimental results that relate to a core-hole initial state and a two-hole valence-electron final state. That AES does indeed give valence data directly relevant to the ground state of molecular species is borne out by a number of observations. Qualitative interpretation of the spectra of CH_3CN has been obtained by using electron-density contours derived from simple Huckel calculations.[14] Secondly, an examination of the Auger intensities in all examples studied to date leads to a chemical interpretation that agrees exceedingly well with valence-electron descriptions given by physical and chemical properties that have been obtained by independent methods. An example is the cycloalkane series[11] mentioned above. ESCA,[47] X-ray/neutron[48-50] diffraction studies of valence electron distributions, and the well-known chemistry of the three-membered strained ring are all consistent with a "bent" bond description, with the maximum C–C bonding electron density not located on the C–C vector but at a point outside the three-membered ring. For cyclopropane, the bonding can be described in terms of sp^2-hybridized carbon

(42) Kelber, J. A.; Jennison, D. R.; Rye, R. R. *J. Chem. Phys.* **1981**, *75*, 652.
(43) Weightman, P.; Thomas, T. D.; Jennison, D. R., *J. Chem. Phys.*, submitted for publication. See also: Thomas, T. D.; Weightman, P. *Chem. Phys. Lett.* **1981**, *81*, 325.
(44) Jennison, D. R.; Kelber, J. A.; Rye, R. R. *Chem. Phys. Lett.* **1981**, *77*, 604.
(45) Assad, W. N.; Burhop, E. H. S. *Proc. Phys. Soc., London* **1958**, *72*, 369.
(46) Shirley, D. A. *Phys. Rev. A* **1973**, *7*, 1520.
(47) Stucky, G. D.; Hedman, J.; Klasson, M.; Nordberg, C.; Matthews, D. *J. Am. Chem. Soc.* **1972**, *94*, 8009.
(48) Matthews, D. A.; Stucky, G. D. *J. Am. Chem. Soc.* **1971**, *93*, 5954.
(49) Coppens, D.; Matthews, D. A.; Stucky, G. D. *J. Am. Chem. Soc.* **1972**, *94*, 8001.
(50) Matthews, D. A.; Stucky, G. D. *J. Am. Chem. Soc.* **1971**, *93*, 5945.

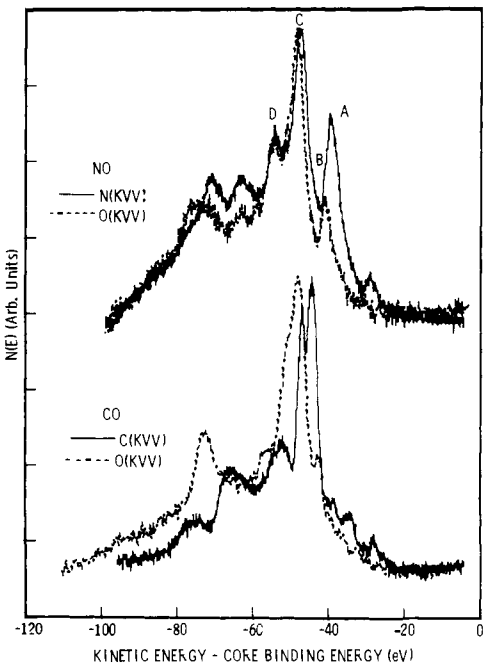

Figure 1. Auger C(KVV) and O(KVV) spectra for CO and N(KVV) and O(KVV) spectra for NO. Plots are made as a function of the two-hole energy = KE − IP(1s). The 1s ionization potentials used are given in Table I.

atoms with the bent bonds the result of $p\pi$–$p\pi$ overlap. AES directly shows this feature and the variation in sp^2 to sp^3 hybridization as one goes through the cycloalkane series from cyclopropane to cyclohexane. The valence-electron polarization for neutral CO and NO as defined by AES will be summarized below.

The relationship of AES to the ground-state charge distributions is evident in the theoretical treatment.[6] Often the initial-state effects of core-hole screening and nonorthogonality work against each other, thus making ground-state charge distribution, multiplied by atomic Auger matrix elements, a good approximation of the actual Auger matrix element.[6] This is true, for example, for the C_2H_6 molecule.[6] For systems such as H_2O[8] in which the shallow valence orbitals react similarly to the presence of the core hole, the *relative* intensities are similar to ground-state predictions.[9] A more detailed treatment of transitions including the problem of nonorthogonality between initial-state and final-state wave functions is contained in the Appendix.

All calculations were performed with the HONDO program[51] and double-ζ or better basis sets.[52] Vibrational broadening was not determined from first principles. In order to *check* the validity of the theoretically predicted vertical transition energies and amplitudes and to account for the effect of overlapping structures, as done previously,[6,7,41,42] normalized Lorentzian functions of approximate empirical widths were added together to generate the smooth theoretical curves of Figures 3 and 6. Empirically, narrow widths are appropriate for shallow valence holes with progressively wider widths for deeper holes. This procedure is obviously a necessary but not sufficient condition to verify the validity of the theoretical results, especially in a larger molecule with many overlapping structures.

Results and Discussion

Introduction. The Auger results for gaseous CO [C(KVV) and O(KVV)] and NO [N(KVV) and O(KVV)] are given in Figure 1. The spectra are plotted against the appropriate two-hole final-state energy so that the relative Auger transition intensities associated with different atomic locations but with the same final states may be directly compared. The two-hole final-state energy is determined by subtracting the appropriate experimentally determined 1s binding energy from the Auger kinetic energy. Table I contains selected ionization potentials used throughout this paper.

Table I. Selected Valence and Core Ionization Potentials (eV)

	CO[b]	NO[b]	$Co(CO)_3NO$[c]	$Fe(CO)_5$	$Mo(CO)_6$
C(1s)	296.2		293.8	293.7[c]	93.2[c]
N(1s)		410.1–411.5 (410.5)	407.8		
O(1s)	542.6	543.1–543.6 (543.2)		540.0[c]	539.6[c]
3σ	38.3	40.6–43.8 (41.4)		35.8[a]	36.5[a]
4σ	19.7	21.7–23.3 (22.1)		18.1[a]	17.9[a]
1π	16.8	15.7–22.0 (17.0)		14.7[a]	13.9[a]
5σ	14.0	16.6–18.3 (17.0)			
2π		9.26			

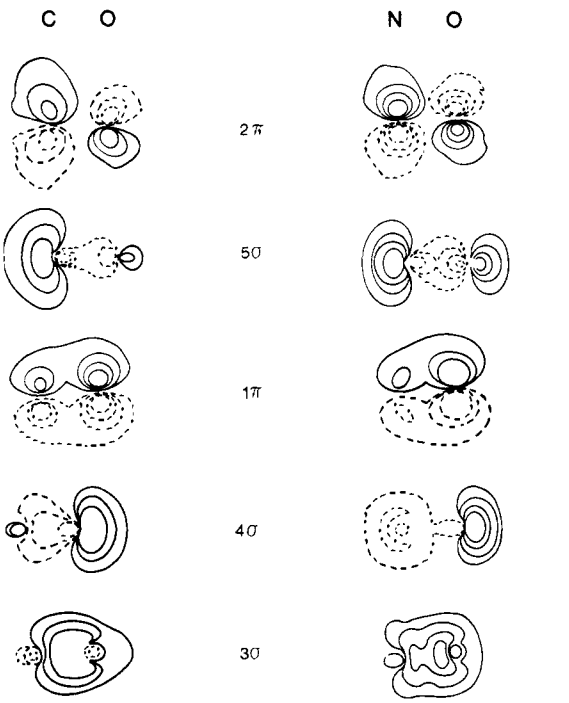

Figure 2. Molecular-orbital contours for CO[25] and NO.[58] Contour values are in atomic units with the lowest value 0.10 and increases in steps of 0.10.

A straightforward comparison of CO and NO is easily made in view of the "aufbau" relationship between the molecules and the known valence ionization potentials.[19,48,54–57] The molecular-orbital contours for CO and NO derived from ab initio calculations[25,58] are given in Figure 2 and can be used to directly illustrate the ability of Auger spectroscopy to define the polarization of the valence electron density distributions for the various molecular orbitals at the atomic sites.

Carbon Monoxide. It is convenient to begin by summarizing the spectra of carbon monoxide as it will form the basis for the rest of our discussion. The experimental and calculated C(KVV)

(51) Dupuis, M.; Rys, J.; King, H. *QCPE* **1977**, *10*, 336.
(52) Dunning, T. H., Jr. *J. Chem. Phys.* **1970**, *53*, 2823.
(53) Plummer, E. W.; Loubriel, G.; Rajoria, D.; Albert, M. R.; Sneddon, L. G.; Salaneck, W. R. *J. Electron Spectrosc. Relat. Phenom.* **1980**, *19*, 35.
(54) Siegbahn, K.; Nordling, C.; Johansson, G.; Hodman, J.; Hodin, P. F.; Hamrin, K.; Gelius, U.; Bergmark, T.; Werme, L. O.; Manne, R.; Baer, Y. "ESCA Applied to Free Molecules"; North Holland: Amsterdam, The Netherlands, 1969.
(55) Davis, D. W.; Martin, R. L.; Banna, M. S.; Shirley, D. A. *J. Chem. Phys.* **1973**, *59*, 4235.
(56) Turner, D. W.; Baker, A. D.; Baker, C.; Brundle, C. R. "Molecular Photoelectron Spectroscopy"; Wiley: London, 1970.
(57) Edqvist, O.; Asbrink, L.; Lindholm, E. *Z. Naturforsch., A* **1971**, *26A*, 1407.
(58) Salahub, D. R.; Messmer, R. P. *J. Chem. Phys.* **1976**, *64*, 2039, and private communication with R. P. Messmer, January, 1981.

Table II. Atomic and Overlap Populations in the Ground and Initial States of CO

	neutral ground state				carbon core hole				oxygen core hole			
MO	C	O	C-O	C/O	C	O	C-O	C/O	C	O	C-O	C/O
5σ	1.88	0.31	−0.19	6.06	1.79	0.17	0.04	10.53	1.97	0.19	−0.16	10.37
1π	0.29	1.34	0.38	0.76	0.59	1.03	0.38	0.57	0.13	1.67	0.21	0.01
4σ	0.38	1.60	0.02	0.24	0.58	1.83	−0.42	0.32	0.34	1.84	−0.18	0.18
3σ	0.20	1.18	0.62	0.17	0.30	1.01	0.70	0.30	0.08	1.55	0.36	0.05

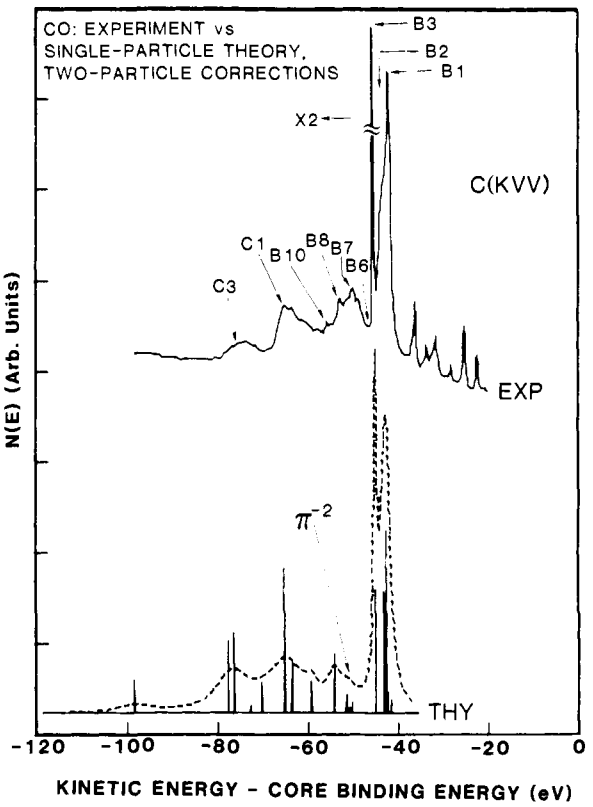

Figure 3. Experimental[59] and calculated[42] C(KVV) Auger spectra for CO. In order to check the validity of the theoretical results, vibrational effects in the experimental spectrum were simulated by broadening the theoretical bar graph using Lorentzian functions of appropriate widths to produce the dotted curve (see ref 42 for details).

Auger line shapes are compared in Figure 3. The high-resolution experimental spectrum is taken from Moddeman et al.[59] A complete assignment of the CO transitions is given in Table I of the supplementary material section and in ref 42. We examine here only the shallow valence (i.e., 2p-like) region of the spectrum, since the one-electron picture has been shown to be less accurate for the ionization of inner valence orbitals, especially in molecules with low-lying virtual levels.[60]

The qualitative relation between the Auger intensities (Figure 1) and the atomic participation in the ground-state molecular orbitals (Figure 2) that make up the Auger states is immediately obvious. For example, one sees a strong carbon KVV contribution from the states derived from the lone-pair orbitals ($5\sigma^{-2}$ and $5\sigma^{-1}1\pi^{-1}$, peaks B3 and B1 in Figure 3, respectively) and a weak Auger intensity for the same transitions in the O(KVV) spectrum,[42] consistent with the 5σ orbital being largely a lone pair localized on the carbon atom. Conversely, the $1\pi^{-2}$ and $4\sigma^{-1}1\pi^{-1}$ intensities (peaks B5 and B7, respectively) suggest a net polarization of these molecular orbitals toward the oxygen atom[42] as predicted by the electron-density contours in Figure 2. Peak B5 is nearly negligible in the C(KVV) spectrum of Figure 3 mainly as a result of configuration interaction[44] with the low-lying virtual 2π orbital but is the dominant peak in the O(KVV) spectrum.[42] Reference 42 should be consulted for details of the CO spectra.

As mentioned, the theoretical analysis predicts that the most important factor that determines the relative intensities of a set of Auger transition is the local, i.e., atomic, charge populations as opposed to other variables including overlap or bonding charge population in the relevant initial-state molecular orbitals.[8,9] Table II compares the Mulliken-orbital population analysis for CO in the neutral ground state and for states with core holes localized on the carbon and oxygen atoms, respectively, in order to consider the effect of the orbital polarization and charge distributions in the neutral parent molecule on the Auger results. The general effect appears to be that bonding orbitals polarize toward the core hole while antibonding orbitals polarize away from the core hole.[6] Differences in the Mulliken populations for the neutral molecule and the initial-core-hole state obviously exist, but information available from AES immediately qualitively defines the molecular-orbital polarizations and quantitatively defines limits for the extent of polarization.

The importance of final-state hole–hole interactions (U_{eff}) to the Auger transition energies is also evident. Valence ionization potentials (Table I) would assign the first transition (the peak with the lowest two-hole binding energy) as $5\sigma^{-2}$ instead of $5\sigma^{-1}1\pi^{-1}$ as given by the theoretical analysis.[42] The $5\sigma^{-1}1\pi^{-1}$ peak has observable intensity in the O(KVV) spectrum but dominates the C(KVV) spectrum so that the transition must involve at least one high-lying bonding orbital with an appreciable amplitude on both the carbon and oxygen atoms but with another high-lying orbital heavily polarized toward the carbon atom. The electronic properties of the $5\sigma^{-1}1\pi^{-1}$ configuration are in agreement with this requirement, results of our calculation,[42] and with the conclusions of Moddeman et al.[59] We also note here that the $5\sigma^{-2}$ peak is extremely sharp, a feature consistent with excitations of the nonbonding and relatively vibration-free 5σ molecular orbital. Theory shows that the reason for the "inverted" state ordering is that the lone-pair character of the 5σ orbital causes the $5\sigma^{-2}$ final state to have a U_{eff} much larger than the $5\sigma^{-1}1\pi^{-1}$ final state (in the latter the holes are largely on opposite ends of the molecule).[42]

Nitric Oxide. The valence ionization potentials for NO and CO are given in Table I, and the Xα-orbital contours of NO and CO are compared in Figure 2. There are a number of significant differences in the charge distributions. The 5σ orbital is nearly equally distributed about the nitrogen and oxygen atoms in NO and no longer qualifies as a lone-pair orbital as in CO. The remainder of the molecular orbitals for NO similarly show a more uniform distribution over the two atomic sites than for CO.

The sensitivity of AES to valence-electron polarization and specifically to these polarization differences between CO and NO is clearly illustrated in Figure 1. There is a large discrepancy in C(KVV) and O(KVV) intensities for several of the Auger transitions of CO in accordance with the polarization of the valence orbitals of CO as discussed above. By comparison, the NO nitrogen and oxygen Auger intensities have more similar Auger profiles consistent with much more uniform valence-orbital distributions.

Because there is only one 2π electron in NO, the $2\pi^{-2}$ transition does not exist. We note that the 1π and 5σ ionization potentials are very similar, having a weighted average of approximately 17 eV (Table I). The 2π ionization potential is roughly 9 eV so that one would anticipate the $5\sigma^{-1}2\pi^{-1}$ and $1\pi^{-1}2\pi^{-1}$ peaks to be shifted by about 8 eV from $5\sigma^{-2}$, $5\sigma^{-1}1\pi^{-1}$, and $1\pi^{-2}$, which is consistent with the separation between the first two low-energy peaks. The

(59) Moddeman, W. E.; Carlson, T. A.; Krause, M. O.; Pullen, B. P.; Bull, W. E.; Schweitzer, G. K. *J. Chem. Phys.* **1971**, *55*, 2317.
(60) Cederbaum, L. S.; Domcke, W.; Schirmer, J.; von Niessen, W.; Diercksen, G. H. F.; Kraemer, W. P. *J. Chem. Phys.* **1978**, *69*, 1591.

Table III. Peak Assignments for the KVV Auger Spectrum of NO

peak	config	calcd int N(KVV)	rel int O(KVV)	two-hole final-state[a] binding energy, eV calcd	exptl	U_{eff}, exptl
A	$5\sigma^{-1}2\pi^{-1}$	51.2	7.5	41.7	40.0	13.7
B	$1\pi^{-1}2\pi^{-1}$	36.2	30.1	42.6	41.5	15.2
	$4\sigma^{-1}2\pi^{-1}$	24.8	5.1	47.2		
C	$5\sigma^{-1}1\pi^{-1}$	95.8	49.8	48.7	48	~14.0
	$1\pi^{-1}1\pi^{-1}$	100[b]	100	50.4[c]		
	$5\sigma^{-1}5\sigma^{-1}$	61.4	11.5	51.3		
D	$4\sigma^{-1}1\pi^{-1}$	37.6	34.0	55.5	~54	~15
	$4\sigma^{-1}5\sigma^{-1}$	56.0	17.0	60.0[d]		
	$4\sigma^{-1}4\sigma^{-1}$	41.2	10.4	60.4		

[a] Due to small amplitudes, triplet states are omitted. [b] May be much too large due to initial state CI effects such as exist in CO; see ref 44. [c] Average of term splittings. [d] May be too large due to neglect of static relaxation; see ref 42.

low-energy peaks therefore can be assigned as $5\sigma^{-1}2\pi^{-1}$ and $1\pi^{-1}2\pi^{-1}$. The valence ionization potentials and the expectation that U_{eff} should not be as large for $5\sigma^{-2}$ in NO as for $5\sigma^{-2}$ in CO would suggest that the $5\sigma^{-2}$ and $5\sigma^{-1}1\pi^{-1}$ transitions make up the largest NO Auger peak. The next highest binding-energy peak would then be derived from $1\pi^{-1}4\sigma^{-1}$ and $5\sigma^{-1}4\sigma^{-1}$.

Theoretical analysis of the NO spectrum confirms these general assignments for the low-energy transitions of NO. The detailed assignments to the experimental peaks labeled in Figure 1 are given in Table III. Peak A in the N(KVV) spectrum is a doublet, as clearly seen in the high-resolution data of Moddeman et al.,[59] with the high-energy peak ($1\pi^{-1}2\pi^{-1}$) of this doublet corresponding to peak B in the O(KVV) spectrum. The low-energy peak of the doublet is not present in the O(KVV) spectrum. This is an exception to the general observation made above that the N(KVV) and O(KVV) Auger line shapes are much more similar for NO than are the C(KVV) and O(KVV) Auger line shapes in CO due to the more uniform electron distribution in NO. The reason for this is partly evident from the orbital contours in Figure 2 and the ground-states charge distribution in Table IV. The 5σ is polarized toward the nitrogen and the 1π toward the oxygen atom, but there is a more even distribution of charge in the 2π so that one would expect the intensity ratio $5\sigma^{-1}2\pi^{-1}$:$1\pi^{-1}2\pi^{-1}$ to decrease in going from the N(KVV) to the O(KVV) spectrum. This is consistent with the calculated intensities in Table IV; however, the observed change in this direction is larger than expected.

The 6σ orbital is of the correct symmetry to mix with the 5σ orbital by configuration interaction and is also strongly polarized toward the oxygen atom. Following the configuration interaction analysis carried out for CO,[42,44] one arrives at the conclusion that the intensity ratio for ($5\sigma^{-1}2\pi^{-1}$):($1\pi^{-1}2\pi^{-1}$) for the O(KVV) will be somewhat reduced by the CI mixing. This is the most likely explanation for the small intensity of the oxygen $5\sigma^{-1}2\pi^{-1}$ transition. Similar considerations suggest that the N(KVV) $1\pi^{-2}$ amplitude of Table III may also be too large due to mixing with the 2π orbital.

Of interest to chemists are the consequences of core-hole formation on the polarization of a given molecular orbital. Does the electronic polarization of the initial state have any relation to the ground-state polarization? The charge distributions for CO and NO (Tables II and IV) show that with one exception the polarization, as given by the ratio of the orbital charges on the atoms forming a bond, is enhanced by core-hole formation at the atom with the largest orbital charge. This enhancement can always be expected to occur in bonding orbitals and as indicated is also observed in the antibonding orbitals of CO and NO with the exception of the 2π NO orbital. In this case the correct polarization for the ground state is still observed as a consequence of the larger nitrogen:oxygen 2π charge ratio for the oxygen core hole and the configuration interaction described previously. The above observations mean that one can comfortably anticipate, as we have concluded previously, that AES will give directly reliable indications of the nature of the valence-electron polarization for the ground-state molecule. Quantitative evaluation of the magnitude of this polarization requires a detailed theoretical analysis.

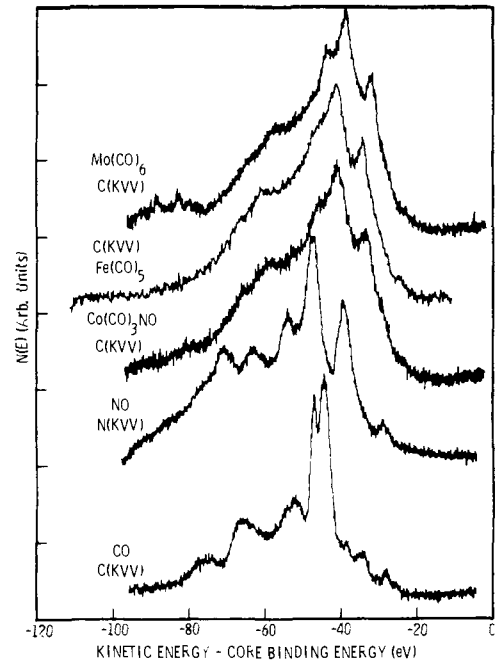

Figure 4. C(KVV) Auger spectra for $Mo(CO)_6$, $Fe(CO)_5$, $Co(CO)_3NO$, and CO, and the N(KVV) spectrum for NO. The Auger intensity is plotted against the two-hole energies. Core ionization potentials given in Table I.

Recently, an analysis of the NO Auger spectrum by Ågren[61] has appeared, which yields calculated transition energies in general agreement with the present work. However, the amplitude differs somewhat, probably due to the neglect by Ågren of screening and nonorthogonality effects.[6] Reference 61 was discussed further in a recent review.[41] We note that our amplitude treatment, coupled with assignments taken from an energy analysis, correctly predicts the variations in amplitude (relative to peak C) of peaks A, B, and D observed when comparing the N and O spectra in Figure 1.

Transition-Metal Carbonyls and Nitrosyls. A number of workers have used Auger spectra to identify and characterize CO reaction intermediates on metal surfaces. The Auger line shapes have been found to be useful for studying surface reactions such as the electron-beam-induced decomposition of adsorbed CO,[62] distinguishing between graphite-like overlayers and surface carbides on metal surfaces, and differentiating between different carbon-containing gases adsorbed by metal surfaces.[63] In general, a variety of C and O Auger spectral differences were found by Hooker and Grant on clean, ion-bombarded transition-metal surfaces.[64] The use of these differences in Auger spectra to identify catalytically important carbon species produced initially by in situ CO reactions on metal surfaces has been explored by Goodman et al.[35] It is clearly important for the above applications to have as thorough an understanding as possible about the origin of the changes observed in the Auger line shapes of CO as it is chemisorbed or bonded to a transition metal.

The C(KVV) Auger spectra of gas-phase $Mo(CO)_6$, $Fe(CO)_5$, and $Co(CO)_3NO$ and CO are shown in Figure 4 along with the N(KVV) spectra for NO. The portion of the spectra of greatest importance from a chemical point of view is the low-binding-energy or outer-valence region. In this respect, the most substantial difference between the Auger spectra of free CO and that of the various metal carbonyls is the appearance (noted also in ref 19)

(61) Ågren, H. *J. Chem. Phys.* **1981**, *75*, 1267.
(62) Haas, T. W.; Grant, J. T.; Dooley, G. J. *J. Appl. Phys.* **1972**, *43*, 1853.
(63) Chesters, M. A.; Hopkins, B. J.; Jones, A. R.; Nathan, R. *Surf. Sci.* **1974**, *45*, 740.
(64) Hooker, M. P.; Grant, J. T. *Surf. Sci.* **1977**, *62*, 21.

Table IV. Atomic and Overlap Populations in the Ground and Initial States of NO

	neutral ground state				nitrogen core hole				oxygen core hole			
MO	N	O	N–O	N/O	N	O	N–O	N/O	N	O	N–O	N/O
$2\pi^a$	0.25	0.16	−0.16	1.56	0.17	0.17	−0.09	1.0	0.25	0.07	−0.09	3.57
5σ	1.34	0.74	−0.08	1.81	1.42	0.53	0.05	2.68	1.53	0.56	−0.09	2.73
$1\pi^a$	0.47	1.14	0.38	0.41	0.85	0.83	0.33	1.02	0.20	1.58	0.21	0.13
4σ	0.98	1.27	−0.26	0.77	1.15	1.61	−0.76	0.71	0.95	1.61	−0.56	0.59
3σ	0.38	0.96	0.67	0.40	0.48	0.83	0.69	0.58	0.20	1.28	0.52	0.16

[a] Charge populations are for one of the degenerate π orbitals.

Table V. CO and NiCO Electron Charge Distributions[a]

			ground state					auger initial state, $C1s^{-1}$					auger initial state, $O1s^{-1}$				
MO		I	Ni	Ni–C	C	C–O	O	Ni	Ni–C	C	C–O	O	Ni	Ni–C	C	C–O	O
CO	5σ	14.0			1.88	−0.19	0.31			1.79	0.04	0.17			1.97	−0.16	0.19
	1π	16.8			0.29	0.38	1.34			0.59	0.38	1.03			0.13	0.21	1.67
NiCO	$3d\sigma$	8.5	1.95	0.02	0.04	−0.01	0.02	1.92	−0.07	0.15	−0.01	0.02	1.83	0.01	0.17	−0.04	0.04
	$3d\pi$	8.5	1.86	0.06	0.03	−0.04	0.11	1.54	−0.07	0.15	−0.01	0.35	1.58	0.19	0.24	−0.11	0.11
	5σ	13.9	0.25	0.50	0.98	0.02	0.30	0.11	0.14	1.01	0.13	0.62	0.25	0.30	1.36	−0.07	0.16
	1π	14.8	0.01	0.00	0.33	0.39	1.26	0.02	0.02	0.63	0.39	0.94	0.00	−0.01	0.14	0.23	1.64

[a] Orbital populations are normalized on two electrons per orbital, although only nearest-neighbor overlap populations are shown. The Auger matrix elements are directly sensitive to the atomic charge due to the small size of interatomic contributions (ref 10). I = ionization potential used in eq 1. Orbitals in NiCO are labeled by their parentages since the mixing is not large in the ground state. Note that the 1π orbital is practically unaffected by the presence of the metal atom. While some workers have found more backbonding than these results (ref 40), others (ref 27, 30) essentially agree with the present work, while others find less (ref 25, 66). The "amount" appears to critically depend upon the method of population analysis and the quality and details of the set used.

of a relatively large low-energy (~−34 eV) peak in the carbonyls, which presumably corresponds to transitions involving the HOMO that has appreciable density at the carbon site. A comparison of the differences between the NO N(KVV) and CO C(KVV) Auger spectra with those between the C(KVV) spectra of CO and the metal carbonyls suggests that the low-binding-energy metal carbonyl peak may be due to an Auger transition involving an orbital that mixes in 2π character. Analogous to NO, the first peak and its low-binding-energy shoulder would then correspond to the "$2\pi^{n-1}5\sigma^{-1}$ and "$2\pi^{n-1}1\pi^{-1}$ transitions and the intense peak at ~40 eV to $5\sigma^{-1}1\pi^{-1}$. Here by "2π" we mean the bonding $d\pi + 2\pi$ orbital and will refer to this level henceforth as the $d\pi$ level since its parentage is predominantly $d\pi$. It has been suggested that the most probable Auger initial state on metal surfaces may not be the adiabatically relaxed state but may have a shakeup configuration.[65] If by analogy this is also true in the molecular case, the above-mentioned low-energy peak may involve the shakeup electron and thus have a different interpretation. We distinguish between these possibilities below.

Further analysis requires a comparison in some detail of the variations in peak positions as observed for the metal carbonyls vs. CO (Figure 4). Reference should also be made to Figure 5, which compares the carbon (KVV) and oxygen (KVV) Auger spectra for $Fe(CO)_5$ and CO, and to the binding energies given in Table I for CO and the carbonyls. It is clear from this comparison that except for the new peak at ~−34 eV, there is a close correspondence in both the C(KVV) and O(KVV) spectra between CO and the metal carbonyls. Comparing the O(KVV) spectra in Figure 5, only a 3-eV shift is required to bring the spectra into excellent agreement. Our assignment of the −40-eV peak in the metal carbonyls to the $5\sigma^{-1}1\pi^{-1}$ final state would suggest that most of this shift is due to the energy differences of the corresponding valence levels between the two molecules. The difference between the sum of the 5σ and 1π binding energies (the $5\sigma^{-1}1\pi^{-1}$ two-hole energy, ignoring U_{eff}) for CO and $Mo(CO)_6$ from Table I is 3.0 eV while the experimental value from Figure 4 is ~5.0 eV. Although there is considerable uncertainty in the energies of the carbonyl 5σ and 1π levels (the 5σ and 1π photoelectrons are unresolved in ref 19), this analysis does suggest that to a first approximation one can view the carbonyl spectra as perturbed CO spectra.

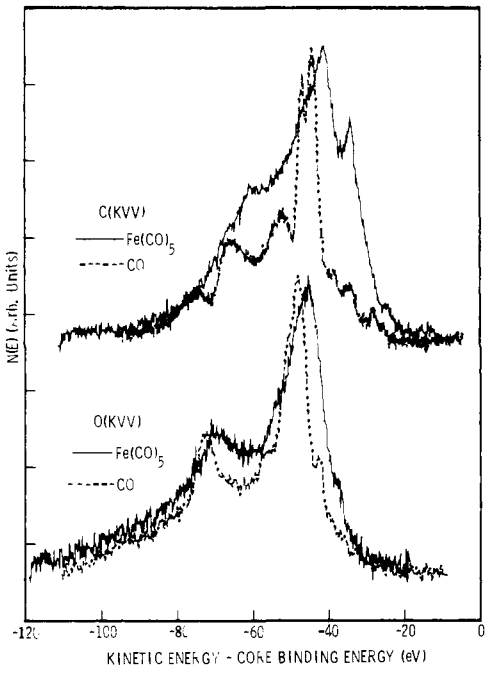

Figure 5. Comparison of C(KVV) and O(KVV) Auger lines for $Fe(CO)_5$ and for CO. Auger intensities are plotted against the two-hole energies. Obtained with core ionization potentials from Table I.

The above experimental comparison also suggests that the values of U_{eff} for CO are at most only slightly decreased (2–3 eV) upon complexation. These results strongly support the conclusion[36] that the final-state holes for those states producing the valence features are localized on one CO ligand, since Coulomb-interaction integrals show that delocalization of the Auger holes over the entire molecule would result in a large decrease (with respect to CO) in the value of U_{eff} (by ~7 eV) and a consequent shift of the carbonyl C(KVV) and O(KVV) spectra to higher energy. In view of this and the fact that the observable differences in the outer-valence transitions are explainable in large part in terms of the valence ionization potentials, it is appropriate and convenient to theoretically analyze the spectra by using localized orbitals generated by a computationally simple model carbonyl, Ni(CO). These results are given in Figure 6 and Tables V and VI.

(65) Bagus, P. S.; Hermann, K. *Surf. Sci.* **1979**, *89*, 588.

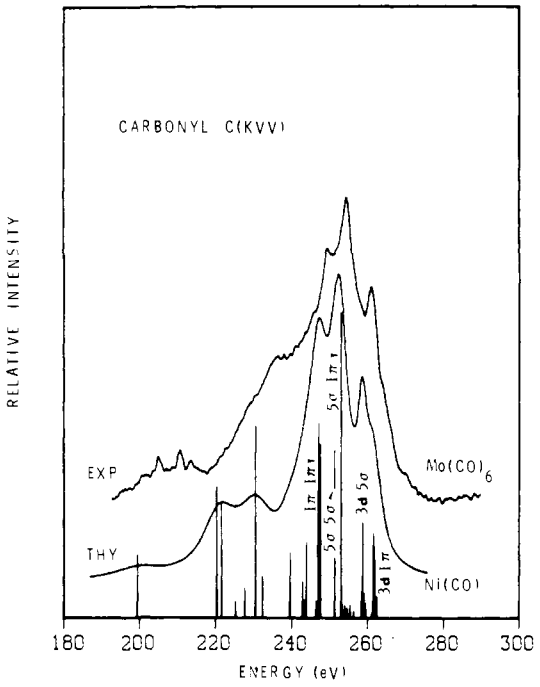

Figure 6. Theoretical spectra for Ni(CO) and observed line shapes for $Mo(CO)_6$.

Table VI. Calculated Transitions for the C(KVV) Auger Decay of Nickel Carbonyl

hole config	relative intensity singlet	relative intensity triplet	U_{eff}(S),[a] eV	energy(S),[a] eV	energy (exptl), eV
$3\sigma^2$	0.205		22.3	199.2	
$3\sigma 4\sigma$	0.430	0.053	19.2	220.3	
$3\sigma 1\pi$	0.379	0.099	21.0	221.5	
$3\sigma 5\sigma$	0.628	0.136	13.1	230.3	
$4\sigma^2$	0.212		18.2	239.3	
$3\sigma 3d\pi$	0.118	0.030	6.3	242.7	
$3\sigma 3d\sigma$	0.059	0.012	5.8	243.0	
$4\sigma 1\pi$	0.246	0.053	16.9	243.6	
$1\pi^2$	0.906[b]	0.000	16.7	246.8[c]	249.0
$4\sigma 5\sigma$	0.638	0.050	14.5	246.9	
$5\sigma^2$	0.549		15.2	250.1[d]	
$1\pi 5\sigma$	1.000[e]	0.040	11.7	252.7	255.0
$3d\pi^2$	0.074	0.000	21.4	254.4[c]	
$3d\sigma 3d\pi$	0.021	0.001	20.1	256.0	
$3d\sigma^2$	0.003		19.6	256.5	
$5\sigma 3d\sigma$	0.087	0.000	10.8	259.9	
$5\sigma 3d\pi$	0.314	0.012	10.5	260.2	261.0
$4\sigma 3d\pi$	0.078	0.017	6.3	260.5	
$4\sigma 3d\sigma$	0.048	0.003	5.7	261.1[c]	
$1\pi 3d\pi$	0.507	0.000	6.6	263.4	264.0
$1\pi 3d\sigma$	0.068	0.004	5.6	264.0	(shoulder)

[a] Due to small triplet amplitudes, only singlet values are given. [b] This value may be altered by initial state CI (ref 44). [c] Average of term values. [d] This value low by ~1 eV due to neglect of static relaxation (ref 42). [e] Normalized on highest amplitude transition. Major shallow transitions are underlined.

The localization we have just described is consistent with the concept[38-40] that localization of the two holes will occur when the strength of the screened hole–hole interaction is such that the difference in energy of a configuration of two holes on one ligand compared to holes separated on two ligands (ΔU) is large compared to the relevant splittings of single-hole energies (W). In the present molecular case, $W_{5\sigma}$ and $W_{1\pi}$ are the spreads due to the interaction of equivalent 5σ and 1π group orbitals, respectively, and may be found from MO theory.[28] Since $\Delta U/W$ here is about 5/1,[36] localization is expected.

There is one other interesting point concerning the changes in the C(KVV) Auger line shapes for CO upon complexation. The

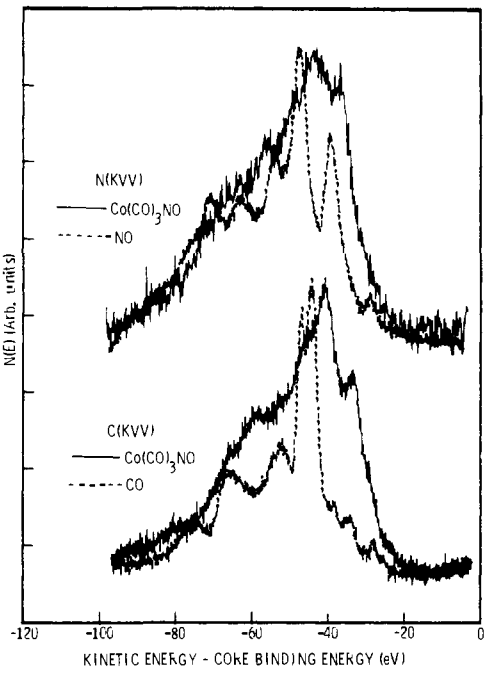

Figure 7. N(KVV) and C(KVV) Auger spectra for $Co(CO)_3NO$, NO, and CO plotted on a two-hole energy scale with core ionization potentials from Table I.

carbon atom 5σ population decreases from 1.79 in CO to 1.01 in Ni(CO) for the $C1s^{-1}$ core-hole state (Table V) so that the intensities of the $5\sigma^{-2}$ and $5\sigma^{-1}1\pi^{-1}$ transitions relative to states not involving the 5σ orbital are expected to decrease. Since the spectra are normalized to the largest peak, the smaller, high-binding-energy peaks appear larger with respect to the $5\sigma^{-2}$ and $5\sigma^{-1}1\pi^{-1}$ peaks in the carbonyl spectra than in the spectrum of CO (Figure 5). In contrast, the 1π oxygen Auger initial-state population is unchanged in going from CO (1.67) to NiCO (1.64), consistent with more uniform relative intensities in the O(KVV) spectra of CO and the carbonyls (Figure 5).

Published theoretical predictions of the π-backbonding/σ-donation ratio vary widely.[66-68] Our results from ab initio restricted-Hartree–Fock calculations indicate π backbonding of 0.2 e per CO (or 0.1 e for each π orbital) and σ donation of 0.5 e per CO for our basis set.[52] These numbers approximately agree with Fenske–Hall results.[30] Populations relevant to our discussions of the trends in charge transfer (not absolute population) can be found in Table V. Upon the introduction of the carbon core hole (as seen in Table V), almost an entire electron is transferred to the CO. The predominantly $3d\sigma$ and $3d\pi$ orbitals have a sufficiently small ground-state charge density on CO for them to be almost unobservable in an Auger decay originating on the ligand. However, the Auger initial-state populations indicate that a decay producing one hole in a predominantly 3d orbital and one on the ligand should be clearly visible in the C(KVV) spectrum, and also, though with considerably less relative intensity, in the O(KVV) spectrum (note relative populations in Table V and recall that the Auger amplitudes are proportional to the product of the populations). The increase in the Auger initial-state π backbonding is therefore the source of the large magnitude of the high-energy feature of the C(KVV) spectrum, which is thus an example of a backbonding-assisted interatomic Auger decay. The oxygen Auger decay, however, is dominated in the metal carbonyl by the same orbitals (4σ and 1π) as in free carbon monoxide.

If one substitutes nitrogen for carbon and forms the NO complex as in $Co(CO)_3NO$, a number of observations can be made. In Figure 7 the N(KVV) spectra of NO and $Co(CO)_3NO$ as well

(66) See: refs 30 and 31 and included references.
(67) Rosen, A.; Baerends, E. J.; Ellis, D. E. *Surf. Sci.* **1979**, *82*, 139.
(68) Walsh, S. P.; Goddard, W. A., IV. *J. Am. Chem. Soc.* **1976**, *98*, 7908.

as the C(KVV) spectra of CO and $Co(CO)_3NO$ are compared on a common two-hole energy scale. First, the conclusion arrived at in the above discussion concerning the comparison of CO and NO can be used as a starting point. The $d\pi^{-1}5\sigma^{-1}$ and $d\pi^{-1}1\pi^{-1}$ N(KVV) peaks for $Co(CO)_3NO$ and NO are centered at two-hole binding energies of $\sim$−37.5 and $\sim$−40 eV, respectively. Although the valence ionization potentials are not experimentally well-defined,[67] it would appear that the hole–hole repulsion, as in the case of the carbonyls and CO, changes only slightly in going from free to coordinate NO and that the changes in the nitrosyl Auger line shapes can be accounted for by the changes in the valence ionization potential. The $d\pi^{-1}5\sigma^{-1}$, $d\pi^{-1}1\pi^{-1}$ transition is larger for coordinated NO than for coordinated CO, as expected in view of the higher electronegativity of NO. Note, however, that the enhanced relative intensity of this peak upon coordination again is consistent with π backbonding. The apparent decrease in the largest peak, $5\sigma^{-2}$ and $5\sigma^{-1}1\pi^{-1}$, analogous to that observed for C(KVV) in coordinated CO, corresponds to the greater charge transfer that is possible for these orbitals upon core-hole formation when large π backbonding is possible.

We finally note that the level of agreement between carbonyl theory and experiment shown in Figure 6 implies that the initial-state configuration was correctly assigned, i.e., that the dominant initial state is the adiabatically relaxed state. Using our antibonding 2π–$d\pi$ orbitals, we find that a change of initial-state configuration to a low-lying shakeup state occupying this orbital[65] would alter the relative Auger decay probability for $3d^{-1}$ ($1\pi^{-1}$ or $5\sigma^{-1}$) state creation by a factor of at least 2.4. However, if this antibonding orbital were occupied, it would also provide a spectator electron for the $5\sigma^{-1}1\pi^{-1}$ transition and the lower states of Figure 6 but not for the higher states. Our calculations of hole–hole repulsion show that this would shift the energy of $5\sigma^{-1}1\pi^{-1}$ relative to $3d^{-1}5\sigma^{-1}$ and $3d^{-1}1\pi^{-1}$ by $\sim$10 eV, thus destroying the agreement in Figure 6. Thus the observed magnitude of the "interatomic" decay in the carbon spectrum and the relative energies of the final states both argue against the dominance of the shakeup initial state. This is in agreement with a recent detailed analysis of this question by Freund and Plummer.[69]

Auger spectroscopy yields characteristic C(KVV) and O(KVV) fingerprint spectra, which apparently depend primarily on the CO ligand independent of the central metal atom. Comparable C(KVV) spectra have been obtained for $Ir_4(CO)_{12}$[70] and $W(CO)_2$.[19] While our O(KVV) data is limited, Plummer, Salaneck, and Miller report a more extensive set: $Cr(CO)_6$, $Ru_3(CO)_{12}$, $W(CO)_6$, $Fe_2(CO)_9$, and $Ir_4(CO)_{12}$.[19] Although some differences exist in the fine structure, this set of X-ray-excited O(KVV) spectra (obtained both in the solid and gas phases) shows basically the same fingerprint spectrum as in Figure 5. A few scattered reports suggest that the same fingerprint, and therefore similar bonding, is obtained for chemisorbed CO and NO.[2,47,71,72]

Summary

Auger spectroscopy yields a uniquely local view of the valence electrons in molecules. For the metal carbonyls this leads to several conclusions:

(1) The involvement of the 2π level of CO in metal carbonyl bonding is shown to lead to electron density observable at the carbon site as a result of ground-state population and screening of the initial core hole. Theoretical calculations separate the ground-state and screening components.

(2) A common C(KVV) fingerprint spectrum is shown to exist for all carbonyls studied to date and can be qualitatively interpreted in terms of ground-state orbitals of CO.

(3) The two-hole final state (double ion) is shown to remain localized on the atom containing the initial core hole.

(4) As a result of these local characteristics, the Auger spectra of the metal carbonyls, in general, can be described by a detailed theoretical analysis in terms of a model metal carbonyl fragment, NiCO.

(5) The differences between the C(KVV) and O(KVV) spectra of CO and the N(KVV) and O(KVV) spectra of NO are shown to reflect differences in binding energies and orbital-electron-density distributions in the two molecules.

(6) Valence charge densities produced by restricted-Hartree–Fock calculations with double-ζ-accuracy basis sets results in agreement between experimental and theoretical Auger amplitudes. Since the relative amplitude of one of the Auger features is directly proportional to the amount of initial-state backbonding, it is probable that these calculations correctly reproduce the ground-state charge density as well.

Appendix

Auger Transition Probabilities. The core-hole initial state and two-hole final states are described by

$$\Psi_i = N'\cdot\det|\bar{\phi}_c\phi_1' \ldots \phi_j'\phi_k' \ldots \phi_n'\bar{\phi}_a| \quad \text{(A1)}$$

and

$$\Psi_f = N\cdot\det|\phi_c\phi_1 \ldots \bar{\phi}_j\bar{\phi}_k \ldots \phi_n\phi_a| \pm \text{other determinants} \quad \text{(A2)}$$

respectively, where the bars indicate holes, the N are normalization coefficients, $\{\phi_n\}$ and $\{\phi_n'\}$ are molecular orbital basis functions, and the primes indicate molecular orbitals relaxed in response to the core hole. The coefficients c and a denote core and continuum wave functions, respectively.

The two sets of molecular orbitals $\{\phi_n\}$ and $\{\phi_n'\}$ are nonorthogonal so that matrix elements between them involve all permutations of orbitals. This evaluation is carried out by construction of a pseudo final state

$$\Psi_f' = N\cdot\det|\phi_c\phi_1' \ldots \bar{\phi}_j'\bar{\phi}_k' \ldots \phi_n'\phi_a| \pm \text{other determinants} \quad \text{(A3)}$$

which differs from Ψ_i by just two spin orbitals. The pseudo-transition matrix element is thus given by[8]

$$M_{jk}' \propto J_{jk}' \pm K_{jk}' \quad \text{(A4)}$$

which can be found in terms of the sum (singlet states) or difference (triplet states) of the Coulomb and exchange integrals

$$J_{jk}' = K_{kj}' = (ca|j'k') = \int\int \phi_c^*(1)\phi_a^*(2)\frac{e^2}{r_{12}}\phi_j'(1)\phi_k'(2)\,d(1)\,d(2) \quad \text{(A5)}$$

In the LCAO approximation, interatomic contributions to M_{jk}' have been shown to be negligible[10] so that

$$M_{j,k}' \propto \sum_{\mu\nu} c_{j\mu}'c_{k\nu}'(ca|\mu\nu) \pm \text{exchange terms} \quad \text{(A6)}$$

where the sum is over all basis functions on the core-hole site and $c_{j\mu}'$ and $c_{k\nu}'$ are the expansion coefficients of the initial-state molecular orbitals over the basis functions.

The true transition matrix elements (M_{jk}) are calculated from

$$M_{jk} = \sum_{lm} C_{jklm}M_{lm}' \quad \text{(A7)}$$

where

$$C_{jklm} = \langle\Psi_f'(lm)|\Psi_f(jk)\rangle \quad \text{(A8)}$$

The coefficient C_{jklm} is zero unless l and m are orbitals that are occupied in the initial state.

The transition matrix elements and Auger amplitudes are thus related to three factors: (1) the atomic-like matrix elements over the basis set $(ca|\mu\nu)$; (2) the initial-state charge densities on the site with the core hole, $c_{j\mu}'c_{k\nu}'$; and (3) the projection of the initial states upon the final states (eq 7).

Registry No. CO, 630-08-0; NO, 10102-43-9; $Co(CO)_3NO$, 14096-82-3; $Fe(CO)_5$, 13463-40-6; $Mo(CO)_6$, 13939-06-5.

(69) Freund, H. J.; Plummer, E. W. *Phys. Rev. B: Condens. Matter* **1981**, *23*, 4859.
(70) Netzer, F. P.; Bertel, E.; Matthew, J. A. D. *J. Electron Spectrosc. Relat. Phenom.* **1980**, *18*, 199.
(71) Fuggle, J. C.; Umbach, E.; Menzel, D. *Solid State Commun.* **1976**, *20*, 89.
(72) Umbach, E.; Kulkarni, S.; Feuhnerr, P.; Menzel, D. *Surf. Sci.* **1979**, *79*, 1.